ISSN: 2277-3754
ISO 9001:2008 Certified
International Journal of Engineering and Innovative Technology (IJEIT)
Volume 3, Issue 12, June 2014

Train accurate localization using ultra wide band radio and time reversal

B. FALL, F. Elbahhar, M. Heddebaut and A. Rivenq
University of Valenciennes (UVHC), French institute of science and technology for transport, development and networks (IFSTTAR)-France

Abstract*— In guided transport, the precise localization of trains is vital for nominal operation of the transport system. In a propagation environment such as a railway line, an effective localization sensor is complex to design since it must operate in the presence of many fixed and mobile obstacles constituted by the infrastructure and the trains. In order to design a sensor delivering high localization performance, we propose the use of so-called spectral diversity techniques also found under the name of ultra wide band radio. In this work, this radio technique is associated to the time reversal technique, taking advantage of the complex railway propagation environment. The objective is to obtain a reliable and robust localization of rail vehicles by focusing radio signals from a ground balise to the track and, therefore, to the passing train receiving antennas. A theoretical model, simulations and an experimental validation were developed on the properties of energy focusing of time reversal taking into account very different types of environment. Several parameters related to antenna configurations were investigated. The contributions of time reversal to the accuracy of the positioning system are measured by comparing an ultra wide band positioning system alone and then, combining it with time reversal.

***Index Terms*—Train Localization; Balise; Ultra Wide Band Radio; Time Reversal; Railway Infrastructure; Temporal Focusing; Spatial Focusing.**

I. INTRODUCTION

In recent years, operators and users of guided transport systems have expressed a strong demand to provide safe and efficient transport, providing an increasing quality of service. Among all the technical requirements which are consequently generated, it is essential to ensure an adequate exchange of information between vehicles and infrastructure, regardless of the type of application or the propagation environment. In such environments, it is also necessary to allow accurate localization of trains. The rapid development of transport in terms of speed, complexity and diversity of environments generate difficulties to develop such equipment and studies have been performed regarding the optimization of the ground to train communication [1]. Usually, ground to train radio communication exploits access points installed along the track, exchanging data with mobile equipment installed on the trains. Either proprietary radio modems or radio modems derived from existing standards are used. Currently, all these radio modems operate sinusoidal sources of signals occupying radio channels over a limited bandwidth. For the train localization process, drifts of the train odometer, usually composed of a wheel turn counter and a Doppler radar that continuously calculate the position and velocity data, are periodically compensated by ground balises installed between the rails. Balises are working as kilometer-markers and transmit their absolute localization to passing trains. The requested localization accuracy is important and should allow, for example in automated urban subways, vehicles to repeatedly stop in front of station doors, thus, necessitating a few centimeters localization accuracy. This paper proposes a new approach for railway track-to-train short range communication simultaneously providing accurate localization information. Breaking with the recalled conventional approaches, an association between Ultra Wide Band (UWB) radio and Time Reversal (TR) techniques constitutes the heart of the work outlined in this paper. The principle of UWB communication is based on the emission of signals at low power and extremely broad spectra to obtain high flow rates and also facilitate flight time, highly accurate measurements [2]. The TR technique constitutes a focusing technique of the energy radiated by an antenna or multiple transmitting antennas to one or more receiving antennas by the insertion, at the transmitter, of a channel matched filter. The remainder of this paper will now described these techniques, their association applied to the balise, and the results obtained in the context of this railway perspective. It is organized as follows. Section II describes the proposed railway balise and introduces the UWB and TR techniques. Using different configurations, section III develops a theoretical and simulation study of the UWB and TR coupled system. Section IV presents the used experimental TR-UWB setup and the associated experimental results. Finally, conclusions and perspectives are provided in section V.

II. SYSTEM DESCRIPTION

A. New balise proposal

Conventional balises are located between the rails. They have the form of a rectangular parallelepiped, as shown in Fig. 1. The train, passing over the balise, can briefly exchange information with the ground, reads its absolute localization from this track kilometer marker and, therefore, compensates for the drift of its proprioceptive localization sensors.

ISSN: 2277-3754
ISO 9001:2008 Certified
International Journal of Engineering and Innovative Technology (IJEIT)
Volume 3, Issue 12, June 2014

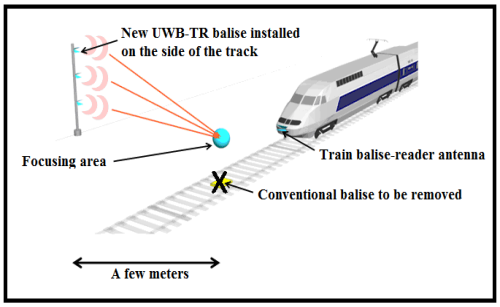

Fig 1. TR-UWB proposed new railway balise

In many railway systems, these balises constitute the only equipment remaining on the track, between the rails, and it could prove worthwhile to remove this last equipment in order to facilitate track maintenance, for example rail replacements. As presented in Fig. 1, in our proposal, the conventional balise situated between the rails is removed and replaced by the new balise, installed on a pole, on the side of the track, and a few meters away. This new balise focuses the radiofrequency energy coming from the pole transmitters to an area situated over the rails, right over the removed conventional balise location. Therefore, this new balise does not interfere anymore with track maintenance operations, but still develop a maximum of radio frequency signal at this particular location over the rails. Several transmitters are coupled on the pole; three can be seen in Fig. 1 to get a multiple source transmitter. This insures transmitter redundancy as well as, when correctly configured, space focusing. One single receiver or train-balise reader is used, located in front of the train. This configuration is usually denoted as a Multiple Input, three transmitters, Single Output, one receiver, MISO 3x1 system. This new balise uses UWB radio associated with TR. UWB radio supports high data rate short range ground to train communication as well as the train localization process. Localization uses time of flight measurements of the received UWB signals from the balise which transmits its own absolute localization. The TR technique helps focusing balise radiation on a small area over the track, represented by a sphere in Fig. 1. When crossing this focusing area, the antenna located in front of the train receives the UWB signals and computes the position to the geo-referenced balise. This system would allow the approaching trains to localize themselves with a very good accuracy. Table 1 establishes a comparison of performance between the communication/localization systems using a railway conventional balise and the expected performance of our proposed TR-UWB balise. This paper evaluates if the expected localization accuracy can be effectively achieved.

TABLE 1. Performance Comparison between a Conventional Balise and The Proposed TR-UWB Balise

	Conventional balise	TR-UWB balise
Operating frequency	27.095 MHz train to ground 4.5 MHz ground to train	3.1 to 10 GHz
Communication range	< 1 m	10 to 100 m
Transmission rates	560 kbps	Potentially up to several hundred Mbps
Localization accuracy expected	20 cm	< 10 cm

Beyond the railway system, this combination of techniques may find application in various areas, such as the detection and localization of persons-through barriers and finding victims of accidents, especially in the mountains or in mines. Through-the-Wall sensing also takes advantage of TR technique; this application is very useful in safety and peace-keeping applications [3].

B. Ultra Wideband radio technique

UWB radio is typically defined as a wireless transmission scheme with a bandwidth of over 500 MHz, or having a fractional bandwidth higher than 0.2 [4]. There are basically two ways of obtaining an UWB signal, using an Orthogonal Frequency-Division Multiplexing (OFDM) approach or, an Impulse Radio (IR) approach. In our study, the second method is chosen. This involves the transmission of very short pulses, typically having time duration of 1 ns or less, therefore, occupying a very wide frequency spectrum. The Gaussian waveform pulse or its derivative are commonly used pulse shapes. Given these characteristics, our choice fell on the UWB technology for the following reasons [5]:

- A transmission capacity up to several hundreds of Mbps has been repeatedly achieved;
- UWB signals have a low probability of non-intentional detection due to the low power spectral density (PSD) used; this property is interesting for secure operation of the transport system;
- The technique provides intrinsically precise localization due to the very short pulses used;
- The communication is robust against the multipath due to the very large bandwidth used;
- UWB signals can share the same frequency bands than other limited bandwidth radio systems, therefore, not involving a dedicated frequency band for the railway application.

The possibility of combining all these capabilities in a single system is a major element that makes UWB a good candidate for communication and localization in guided transportation systems.

Furthermore, radio localization is subject to two major sources of error, the first being the lack of line of sight (*LOS*) between the transmitter and the receiver, and the second being the excessive presence of multipath. The introduction of UWB in wireless communication has brought improvements regarding these sources of errors [6]. However, previous investigations have raised major issues, such as the complexity of the signal processing at the reception [7], [8]. Therefore, UWB has been associated with TR [9], [10],

ISSN: 2277-3754
ISO 9001:2008 Certified
International Journal of Engineering and Innovative Technology (IJEIT)
Volume 3, Issue 12, June 2014

especially in multi-users communication systems, in order to solve part of these problems.

The application of the UWB radio technique to transport is a more recent topic that is thoroughly researched [11] considering several factors including:

- The nature of the transport propagation environment;
- The use of adequate transmitting/receiving duty cycle (LDC);
- The number of collocated used UWB devices;
- The types and levels of interference.

Regulation Bodies have considered these railway applications and Table 2 provides some inputs regarding areas of operation of UWB systems [12].

TABLE 2. Critical Factors Limiting the Performance of UWB Systems in Railway Environment

Frequency (GHz)	Area of Operation	Critical factors impairing system performance	Countermeasures compatible with limits and ECC regulations
3,11 < f < 4,8 PSD <-53,3 dBm/MHz for unregistered UWB unlicensed mobile devices with 5 % activity LDC	very short range (<10 meters)	Multipath Broadband interferers (e.g. automotive UWB)	Multiple UWB emitters onboard the train cars real-time processing Multiple "ground-based" fixed receivers
PSD <-41,3 dBm/MHz for registered devices	short range (<50 meters)	Multipath + path loss Broadband interferers	Multiple UWB emitters at 3,1 GHz to 4,8 GHz deployed as "ground-based" fixed references for real-time processing
6 < f ≤ 8,5 PSD <-53,3 dBm/MHz for unregistered UWB mobile devices with 5 % LDC	very short range (<10 meters)	Multipath	Multiple UWB emitters onboard the train cars real-time processing Narrow-beam antenna
NOTE: At highest frequencies (6 < f ≤ 8,5 GHz) very short-range (<10 meters) applications only are affordable, due to the fact that fixed infrastructures made of UWB emitters are not allowed by ECC.			

C. Time Reversal

Classically, TR has been applied to acoustics and underwater systems [13]. TR is closely related to the retro-directive array in microwave and phase conjugation in optics [14]. The first TR experiment using electromagnetic waves in the 2.45 GHz band was reported by [15]. This contribution suggests that the techniques developed for ultrasound might also be used for the study of electromagnetic case. Indeed, it is an interesting challenge because in many real environments like buildings and confined areas, microwaves, using wavelengths between 5 and 30 cm, are scattered off by objects such as walls, desks, vehicles and so on, which produce a multitude of radio communication paths from the transmitter to the receiver. In such situations, a TR system should be able not only to compensate for the multipath effect, but also to improve radio communication parameters by taking advantage of the energy distributed in the reflected signals [16]. Usually, the following TR process is used. Firstly, the channel impulse response (CIR) is measured between the transmitter (Tx) and the receiver (Rx) and the corresponding Channel State Information (CSI) is then loaded into Tx. Secondly, the selected signal and the impulse response are reversed in time and transmitted by Tx in the propagation channel, up to Rx. This process, represented in Fig. 2, can be mathematically described by noting s(t) the transmitted pulse, h(t) the complex impulse response of the channel and h*(-t) the complex conjugate of the time reversed version of h(t); y(t) the received signal without TR and yRT(t), the received signal with TR at the receiver; one has:

$$y(t) = s(t) \otimes h(t) + n(t) \quad (1)$$

$$y_{RT}(t) = s(t) \otimes h^*(-t) \otimes h(t) + n(t) \quad (2)$$

Where $\otimes$ represents the convolution operation and n(t) is the Gaussian noise. From Eq. (2), we deduce the equivalent impulse response heq(t) which corresponds to the autocorrelation function of the channel:

$$heq(t) = h^*(-t) \otimes h(t) \quad (3)$$

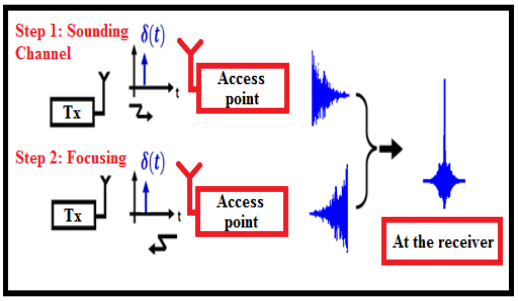

Fig 2. Principle of Time Reversal technique

Applied to our railway balise, this TR general process becomes the following one. The local CSI between any balise transmitter source and the defined focusing defined area, between the rails, is measured or computed a single time during the installation phase of the balise. This CSI information is then loaded in the transmitter equipment to perform the TR operation. As long as the propagation environment remains unmodified, this initial CSI is repetitively used by the balise. This information is then introduced as pre-filtering data in the different UWB transmitters. Therefore, focusing is obtained in the required direction, between the rails, potentially improving the absolute localization process.

A. 1 Parameters to evaluate TR effectiveness

Temporal focusing (TF) that can be observed at the receiver in Fig. 1, and Spatial Focusing (SF) are characteristics associated to TR. To study TF, one can evaluate the Focusing Gain (FG), which is defined as the ratio of the spectrum power of strongest amplitude peak in TR received, to the strongest peak received by a conventional UWB system. The focusing gain can be written as:

$$FG_{[dB]} = 20\log_{10}\left(\frac{\max(|y_{rt}(t)|)}{\max(|y(t)|)}\right) \quad (4)$$

Since the signal level is increased in the receiving area, higher FG could potentially translate into higher communication range and higher precision of localization.

As an example, the study of SF considering a simple transmitter to receiver configuration is performed the following way. The channel impulse response (CIR) of the intended receiver located in position p0 is noted h(p0,t). The CIR of the unintended receiver located in position pi($i \neq 0$) is noted h(pi, $i \neq 0$). The equivalent CIR of the intended receiver

ISSN: 2277-3754
ISO 9001:2008 Certified
International Journal of Engineering and Innovative Technology (IJEIT)
Volume 3, Issue 12, June 2014

is then given by:

$$heq(p_0,t) = h^*(p_0,-t) \otimes h(p_0,t) \quad (5)$$

While the equivalent impulse response of the unintended receiver is given by:

$$heq(p_{i,i\neq 0},t) = h^*(p_0,-t) \otimes h(p_i,t) \quad (6)$$

SF is then evaluated as the ratio of the strongest peak power received by the intended receiver to the strongest peak received by the unintended receiver. The SF parameter can be written as:

$$SF_{[dB]} = 20\log_{10}\left(\frac{\max(|heq(p_0,t)|)}{\max(|heq(p_1,t)|)}\right) \quad (7)$$

III. EVALUATION OF THE TR CHARACTERISTICS IN A MULTI-ANTENNA CONFIGURATION

In Fig. 1, the railway balise uses a MISO 3x1 configuration. We evaluate the contribution of TR in this configuration using the Power Delay Profile (*PDP*) and then computing FG and SF. Firstly, their expressions are determined in the general case of a MISO nx1 configuration then, the analytical and simulation results are presented for cases MISO 2x1 and 3x1. The study of PDP and FG is performed for channel models exploiting successively the ray channel approach and the IEEE 802.15.3a channel model, the latter is based on the Saleh Valenzuela formalism [17]. The ray channel model is presented in [11]. It is set by considering a transmitter (Tx) to receiver (Rx) distance d_0. The propagation domain is bounded by a first horizontal surface, infinite, homogeneous and perfectly smooth with a permittivity contrast (Fig. 3). The signals from Tx to Rx undergo reflections on the floor and ceiling, except in the case of the direct path. An analytical computation of all these rays can be performed using some geometrical considerations.

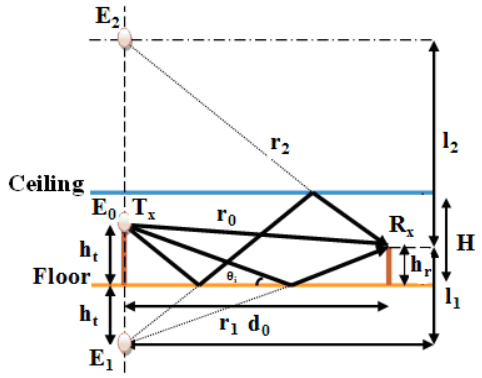

Fig 3. Ray Channel Model

A. Case of ray model

Throughout the development, we denote by:

- $S_i(t)$: the signal transmitted by the i[th] station;
- $h_i(t)$: is the CIR corresponding to the i[th] station;
- * $h_i(-t)$: the conjugate of the CIR corresponding to the i[th] station.

Expression of the impulse response being given by:

$$h_i(t) = \sum_{m=0}^{\infty} \alpha_{mi} s_i(t - t_{mi}) \quad (8)$$

Where m represents the number of paths of the channel, the corresponding amplitude and time of arrival of paths. The general expression for the equivalent impulse response is given by Eq. 9:

$$heq_{MISO}(t) = \sum_{i=1}^{N_t} \int h_i(t) h_i(\tau + t) dt \quad (9)$$

Where N_t is the number of transmit antennas Replacing the expression of $h_i(t)$ in Eq. 9, we get:

$$heq_{MISO}(t) = \sum_{i=1}^{N_t} \int \sum_{m=0}^{\infty} \alpha_{mi} s_i(t - t_{mi}) \alpha_{mi} s_i(\tau + t - t_{mi}) dt$$

$$heq_{MISO}(t) = \sum_{i=1}^{N_t} \sum_{m=0}^{\infty} \alpha_{mi}^2 \int_0^{\infty} s_i(t - t_{mi}) s_i(t + \tau - t_{mi}) dt$$

$$heq_{MISO}(t) = \sum_{i=1}^{N_t} \sum_{m=0}^{N-1} \alpha_{mi}^2 \Phi_{si}(t) \quad (10)$$

Where $\Phi_{si}(t) = \int_0^{\infty} s_i(t - t_{mi}) s_i(t + \tau - t_{mi}) dt$

The PDP is then given by:

$$PDP_{TR-UWB}^{MISO}(t) = |heq_{MISO}(t)|^2 = \left| \sum_{i=1}^{N_t} \sum_{m=0}^{N-1} \alpha_{mi}^2 \phi_{si}(t) \right|^2 \quad (11)$$

Similarly, FG is obtained by considering the power peaks in the case of UWB without TR ($PDP^{MISO}(t)$) and in the case of UWB with RT ($PDP_{TR-UWB}^{MISO}(t)$):

$$FG_{[dB]} = 10Log_{10}\left[\frac{\sum_{i=1}^{N_t} \sum_{m=0}^{N-1} \alpha_{mi}^2}{\sum_{i=1}^{N_t} \alpha_{0i}^2} \right] \quad (12)$$

Fig. 4 (a, b) and Fig. 5 (a, b) illustrate, respectively, the PDP_{TR-UWB} of the MISO 2x1 and MISO 3x1 configurations considering 2 and 10 paths. We observe the strong TF effect. We also note that the amplitude of the PDP increases with the number of paths or the number of antennas. The peak power obtained in the case of MISO 2 x 1 is 0.041 [V^2] for the 2 path channel model, increasing to 0.17 [V^2] for the 10 path channel model. In the case of the MISO 3x1, the respective peak values of the PDP are still higher, 0.08 [V^2] and 0.45 [V^2].

ISSN: 2277-3754
ISO 9001:2008 Certified
International Journal of Engineering and Innovative Technology (IJEIT)
Volume 3, Issue 12, June 2014

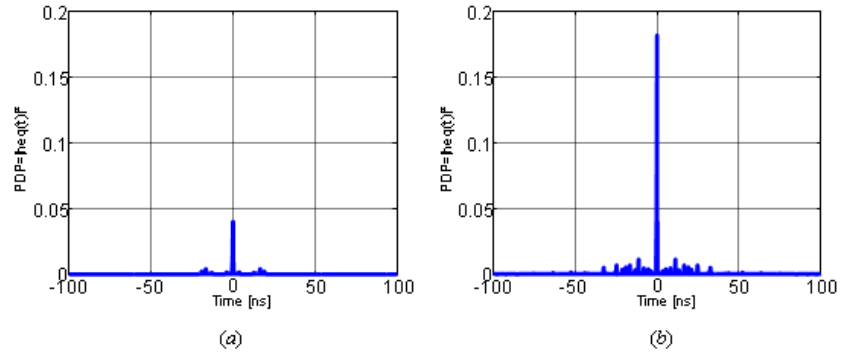

Fig 4. $PDP_{TR\text{-}UWB}$ for MISO 2 x 1 config., a) for 2 path model, b) for 10 path model

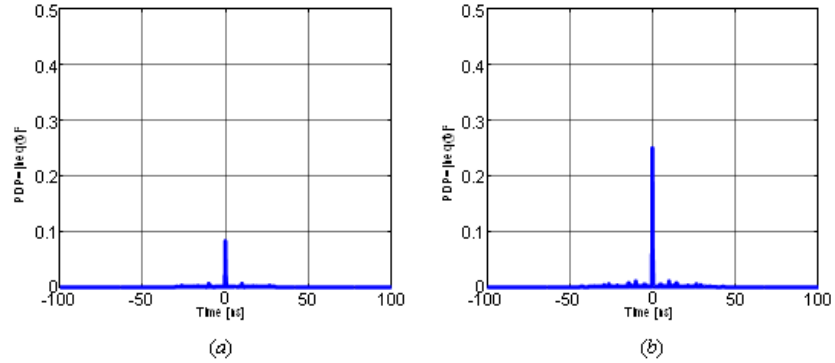

Fig 5. $PDP_{TR\text{-}UWB}$ for MISO 3x1 config., a) 2 path model, b) 10 path model

Table 3 and table 4 represent the focusing gain in the case of MISO 2x1 and MISO 3x1 respectively. This focusing gain is evaluated using successively 2, 4, 6 and 10 paths. We note that the focusing gain increases with the complexity of the channel and the number of transmitters. Indeed, from 2 to 10 paths, the focusing gain increases from 6.0 dB (5.9 dB analytical) to 12.6 dB (12.5 dB analytical), in the case of MISO 2x1 configuration, and from 9.2 dB (9.2 dB analytical) to 16.5 dB (16.5 dB analytical), in the case of MISO 3x1 configuration.

TABLE 3. FG in the Case Of MISO 2x1 Configuration Using 2, 4, 6 And 10 Paths (Analytical and Simulation)

Ray model	2 paths	4 paths	6 paths	10 paths
$FG_{analytcal}[dB]$	5.9	10.2	11.9	12.5
$FG_{simulation}[dB]$	6.0	10.2	12.0	12.6

TABLE 4. FG In The Case Of MISO 3x1 Configuration Using 2, 4, 6 And 10 Paths (Analytical And Simulation)

Ray model	2 paths	4 paths	6 paths	10 paths
$FG_{analytcal}[dB]$	9.2	14.0	15.9	16.5
$FG_{simulation}[dB]$	9.2	14.0	15.9	16 .5

IV. CASE OF IEEE 802.15.3A CHANNEL MODEL

In the case of the IEEE 802.15.3a model, the characteristic values of Nakagami-m were explored, taking into account the number of antennas N_t .

Expression of the CIR is equivalent given by Eq. 13:

$$heq_{MISO}(t) = E\left\{\sum_{i=1}^{N_t} heq_i(t)\right\} \quad (13)$$

Where

$$heq_i(t) = \int_A \sum_{m=0}^{\infty} \alpha_{mi}^2 s_{mi}(\tau - t_{mi}) s_{mi}(\tau + t - t_{mi}) d\tau$$

Then,

$$heq_{MISO}(t) = E\left\{\int_A \sum_{i=1}^{N_t}\sum_{m=0}^{\infty} \alpha_{mi}^2 s_{mi}(\tau - t_{mi}) s_{mi}(\tau + t - t_{mi}) d\tau\right\}$$

$$heq_{MISO}(t) = E\left\{\sum_{i=1}^{N_t}\sum_{m=0}^{\infty} \alpha_{mi}^2\right\}\Phi'_{si}(t)$$

$$heq_{MISO}(t) = \sum_{i=1}^{N_t}\left[E\left\{\sum_{m=0}^{\infty} \alpha_{mi}^2\right\}\right]\Phi'_{si}(t) \quad (14)$$

ISSN: 2277-3754
ISO 9001:2008 Certified
International Journal of Engineering and Innovative Technology (IJEIT)
Volume 3, Issue 12, June 2014

Where $\Phi'_{si}(t) = \int_A s_i(\tau - t_i) s_i(\tau + t - t_i) d\tau$

The calculation of the average energy of the CIR in generic interval $W = [a,b]$ (*a and b are arbitrary chosen*) provides:

$$E\left\{\sum_{i \in I_W} \alpha_i^2\right\} = \int_W P_g(t) dt \quad (15)$$

Where I_W is the random set containing the multipath components.

The variance of the energy function of the CIR is given by:

$$Var\left\{\sum_{i \in I_W} \alpha_i^2\right\} = \int_W R_g(t) dt \quad (16)$$

Where $R_g(t)$ is the kurtosis of the delay profile.

Exploiting Eq. 15 and 16, the expression $heq_{MISO}(t)$ becomes:

$$heq_{MISO}(t) = E_g \sum_{i=1}^{N_t} \Phi'_{si}(t) \quad (17)$$

The corresponding ($PDP^{MISO}_{ULB-RT}(t)$) is given by:

$$PDP^{MISO}_{TR-UWB}(t) = E\left\{heq_{MISO}(t)\right|^2\} \quad (18)$$

After development, Eq. 18 becomes:

$$PDP^{MISO}_{TR-UWB}(t) = \sum_{i=1}^{N_t} \left\{ E_g^2 \Phi'^2_{si}(t) + \frac{E_g^2}{2\tau_{rms}} * \varpi \right\} \quad (19)$$

Where,

$$\varpi = \left[(1 + \Psi_{\Phi'_{si}}(t)) c_{1i} \exp(-t/\tau_{rms}) + (1 + \frac{1}{m'}) \frac{1}{\lambda} \Phi'^2_{si}(t) \right]$$

and,

$$c_{1i} \Psi_{\Phi'_{si}}(t) = \int_{A'} \phi_s(\xi + t) \phi_s(\xi - t) d\xi d\tau,$$

$\Psi_{\Phi'_{si}}(t)$ is the normalized autocorrelation of $\Phi'_{si}(t)$

$\Psi_{\Phi'_{si}}(0) = 1$

The corresponding focusing gain is given by Eq. 20.

$$FG_{[dB]} = 10 Log_{10} \left[\frac{E_g \sum_{i=1}^{N_t} \tau_{rms} + c_{1i} + c_2}{N_t} \right] \quad (20)$$

Where, $c_2 = (1 + \frac{1}{m'}) \frac{1}{2\lambda}$, m' represents the Nakagami-m value.

The values obtained on the evaluation of focusing gain for MISO 2x1 and MISO 3x1 configurations are respectively presented in table 5 and table 6. These values correspond to the different IEEE 802.15.3a Channel Model configurations known as CM1, CM2 and CM3 corresponding to different increasing channel complexities. The same observations are found using this IEEE model than using our previous ray channel model. Indeed, taking the example of MISO 3x1 configuration, changing from CM1 to CM3, FG increases from 14.6 dB to 20.1 dB. The focusing gain is also greater in the MISO 3x1 configuration as compared to the MISO 2x1 configuration.

TABLE 5 . FG in Analytical and Simulation Study, Case Of MISO 2x1 (IEEE 802.15.3a Channel Model)

IEEE 802.15.3a channel model	CM 1	CM 2	CM3
$FG_{analytcal}[dB]$	10 .2	12.9	16.2
$FG_{simulation}[dB]$	10.3	13.0	16.3

TABLE 6 . FG IN ANALYTICAL AND SIMULATION STUDY, CASE OF MISO 3X1 (IEEE 802.15.3A CHANNEL MODEL)

IEEE 802.15.3a channel model	CM1	CM2	CM 3
$FG_{analytical}[dB]$	14.4	16.1	19.9
$FG_{simulation}[dB]$	14.6	16.2	20.1

V. EXPERIMENTAL VALIDATION

The purpose of this experimental validation is to assess the impact of environmental complexity on performance related to temporal/spatial focusing and positioning error, and to compare these conclusions to our preceding simulation results.

A.1. Experimental setup

An Arbitrary Waveform Generator (AWG) associated with a fast sampling oscilloscope (TDS) is used. These equipment have different available ports that can be used to respectively generate and acquire signals. The pulses generated by the AWG are radiated using wideband horn antennas. Similar antennas are used for receiving; their outputs are connected to the TDS ports through low noise amplifiers (LNA). A portable computer is used to process the signals and store the results. We consider two types of environment: an anechoic chamber environment and an indoor environment. In the anechoic chamber, metallic reflectors are introduced to create, on demand, different configurations of multipath. In each type of environment, different geometrical configurations (SISO or MISO) and different locations of the antennas were tested. Therefore, different sets of parameters are implemented to verify the impact of these very different propagation channels on system performance.

A.1.1. Anechoic chamber environment

The dimension of the anechoic chamber we used is 7 x 7 x 3 m, it is operating from 100 MHz to 10 GHz.

Three antennal configurations are considered:

A SISO configuration consists of a single transmitting antenna and a single receiving antenna;

A MISO 2x1 configuration consists of two transmitting antennas and one receiving antenna;

A MISO 3x1 configuration consists of three transmitting antennas and one receiving antenna.

For each type of configuration, five cases are considered:

the anechoic chamber environment type is considered as it,

ISSN: 2277-3754
ISO 9001:2008 Certified
International Journal of Engineering and Innovative Technology (IJEIT)
Volume 3, Issue 12, June 2014

without addition of metal reflectors ;

A single aluminum plate (2 m x 1 m) is introduced as a reflector between transmitters and receiver to generate a first multipath configuration;

Two reflector plates are introduced to increase the number of reflected signals;

Three plates are installed to further increase the number of reflections in the propagation environment;

Four plates are present to maximize the propagation environment complexity.

Fig. 6 presents a view corresponding to this third configuration.

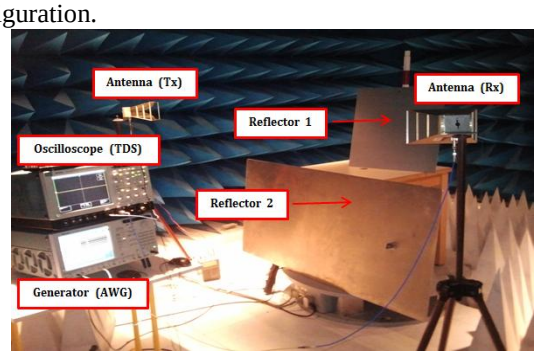

Fig 6. Implementation of third configuration (presence of two reflector plates in SISO)

A.1.2. Indoor environment

We also consider the indoor complex environment shown in Fig. 7. This environment looks like a limited section of tunnel and is subject to multipath propagation. This area presents its own reflections and, therefore, do not necessitate adding supplementary reflectors. Configurations SISO, MISO 2x1 and MISO 3x1 are also selected to evaluate the TR-UWB localization system.

Fig 7. Indoor environment (tunnel type)

A.2. TR focusing effect experimental evaluation

In this section, we experimentally evaluate the TR focusing effect before measuring its impact in terms of positioning errors.

A.2.1. TR focusing in an anechoic chamber environment

Our objective is to evaluate the focusing gain (FG), on the one hand, as the complexity of the propagation channel increases, and, on the other hand, as the antenna configuration evolves from SISO to MISO 3x1. For the SISO configuration, the distance between the transmitting antenna and the receiving antenna is 5 m, which is representative of the railway balise application. The MISO 2x1 configuration is set so as to obtain a distance of 5 m between Tx1 and Rx, and 3.6 m between Tx2 and Rx. MISO 3x1 configuration corresponds to the addition of a third transmitting antenna using a distance of 4 m between Tx3 and Rx. In a first step, for each selected configuration, a pulse is transmitted using the AWG; the received signal is acquired by the TDS, and then returned temporally. In the cases of MISO 2x1 and MISO 3x1, each Tx re-emits its corresponding reversed in time signal. Fig. 8a shows, in the SISO configuration, an example of the received signal without TR. This configuration uses three reflector plates. By comparing it with the corresponding TR signals presented in Fig. 8b, we observe a significant increase in the amplitude of the received signal. To assess this temporal focusing, we calculate the focusing gain (FG) obtained in each case. The overall results are grouped in table 7. We obtain that, for each of the three configurations, the focusing gain increases with the number of reflector introduced. For example, in the case of SISO configuration, FG increased from 2.2 dB with one reflecting plate up to 6.1 dB using four reflector plates. Moreover, by comparing the values of FG for these three types of configuration, we find that FG increases from SISO to MISO configuration. Considering the four reflector scenario, FG is 6.1 dB in the SISO configuration, increasing to 9.8 dB in the MISO 2x1 configuration and reaching 12.8 dB in the MISO 3x1 configuration. These results confirm the benefit of a higher complexity of the propagation environment when using TR. It also demonstrates the interest of using a multi-antenna configuration. They are in good accordance with our simulation results.

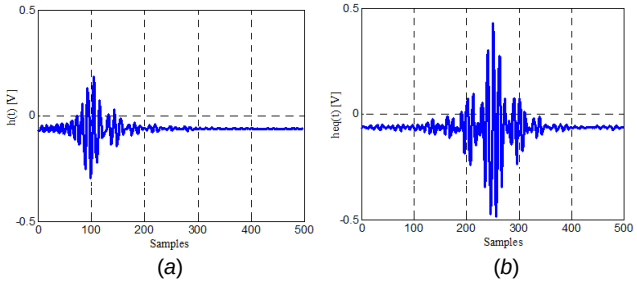

Fig 8. Received signal without TR (case of SISO configuration, with 3 reflector plates), b) Received signal with TR (case of SISO configuration, with three reflector plates)

TABLE 7. FOCUSING GAIN (FG) ACCORDING TO THE NUMBER OF REFLECTOR PLATES INSERTED IN THE PROPAGATION ENVIRONMENT (CASE OF SISO, MISO 2X1 AND MISO 3X1 CONFIGURATIONS)

Configuration	SISO	MISO 2x1	MISO 3x1
$FG_{[dB]}$ (without reflector)	1.0	1.6	1.7
$FG_{[dB]}$ (1 reflector plate)	2.2	3.8	5.9

ISSN: 2277-3754
ISO 9001:2008 Certified
International Journal of Engineering and Innovative Technology (IJEIT)
Volume 3, Issue 12, June 2014

$FG_{[dB]}$ (**2 reflector plates**)	3.2	5.9	8.2
$FG_{[dB]}$ (**3 reflector plates**)	5.1	7.4	9.4
$FG_{[dB]}$ (**4 reflector plates**)	6.1	9.8	12.8

To evaluate SF, we consider the scenario using three reflector plates. For the three SISO, MISO 2x1 and MISO 3x1 configurations, the receiver is moved by 10 cm from its initial position. We note the initial position p0 and p1 the position after displacement. Fig. 9 represents an illustration of the SISO experimentation. The signal previously reversed in time at position p0 is transmitted and this signal is now received at position p1, where the used CSI is no more optimal.

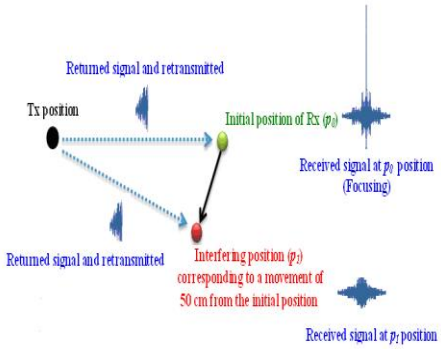

Fig 9. Principle of SF measurement

Fig. 10a and Fig. 10b show an example of the received signals after time reversal for various positions p0 and p1 in a SISO configuration using three reflector plates. We note that, from position p0 to position p1, a loss of focalization is obtained. We then evaluate SF obtained at position p0, compared to SF obtained at position p1, using our three configurations and five reflector scenarios. The results are summarized in table 8. By making a comparison between, on the one hand, the five considered reflector cases, on the other hand, the three types of configuration, we note that SF values increase with the number of reflectors, but also as a function of number of transmitting antennas. This confirms, the results obtained in theory and simulation.

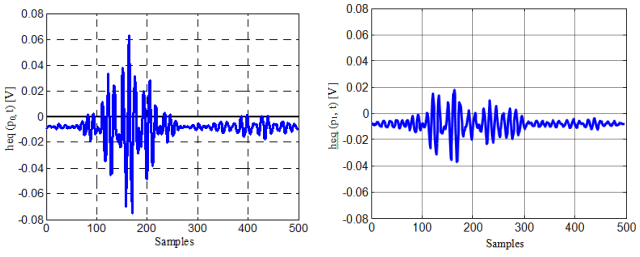

(*a*) (*b*)

Fig 10. a) Received signal at target position p_0 (SISO configuration with 2 reflector plates); b) Received signal at interfering position p_1 (SISO configuration with 2 reflector plates)

TABLE 8 . SF According to the Number of Reflector Plates Inserted in the Propagation Environment

Configuration	SISO	MISO 2x1	MISO 3x1
$SF_{[dB]}$ (**without reflector**)	2.3	2.4	3.1
$SF_{[dB]}$ (**1 reflector plate**)	5.8	6.2	8.1
$SF_{[dB]}$ (**2 reflector plates**)	7.9	9.8	11.1
$SF_{[dB]}$ (**3 reflector plates**)	10.0	11.5	13.2
$SF_{[dB]}$ (**4 reflector plates**)	12.3	14.3	16.4

A.2.2. TR focusing in the indoor environment

The experimental setup, initially installed in the anechoic chamber, is now transferred to the indoor environment seen in Fig. 7. We consider our three SISO, MISO 2x1 and MISO 3x1 configurations and this particular indoor propagation environment. We performed the same measurements as in anechoic chamber to evaluate SF and TF. Fig. 11 (a, b) present respectively, the received signals without TR and with TR for SISO configuration. By comparing the received signals, we observe again the phenomenon of TF. Furthermore, by comparing the amplitudes of signals received with the three configurations, one can observe that the largest amplitude is obtained with the MISO 3x1 configuration, the MISO 2x1 configuration in turn presents a stronger amplitude of the received signal relative to SISO configuration.

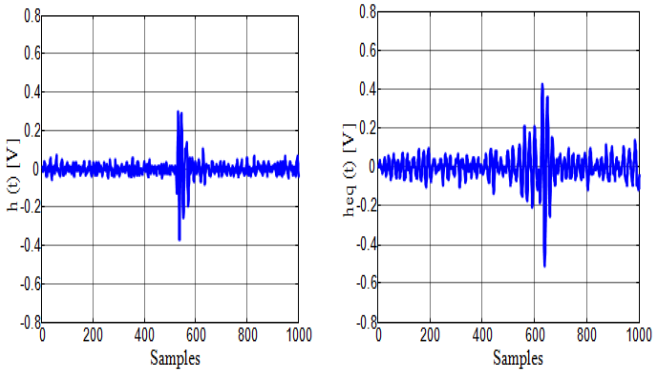

(*a*) (*b*)

Fig 11. a) Received signal without TR, b) Received signal with TR (SISO configuration)

These results reinforced those already obtained on the assessment of FG and presented in Table 6. In the latter, we notice the increasing FG values according to the number of transmitting antennas used. Next, evaluation of the spatial focusing on the target position p_0 compared to p_1 position is performed using our three types of configurations. Fig. 12 (a, b) respectively show the signals received at positions p_0 and p_1, in the case of SISO configuration. We also find a loss of focusing passing from position p_0 to position p_1. Table 10 gives the values of SF for the three types of configurations, corresponding to the displacement relative to p_1 versus p_0.

ISSN: 2277-3754
ISO 9001:2008 Certified
International Journal of Engineering and Innovative Technology (IJEIT)
Volume 3, Issue 12, June 2014

TABLE 9 . FOCUSING GAIN (FG) IN INDOOR ENVIRONMENT (CASE OF: SISO, MISO 2X1 AND MISO 3X1)

Configuration	SISO	MISO 2x1	MISO 3x1
$FG_{[dB]}$ (Laboratory type)	2.9	3.8	5.0
$FG_{[dB]}$ (Tunnel type)	3.8	4.9	6.7

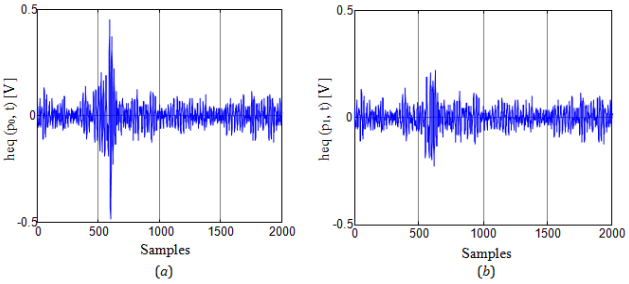

Fig 12. a) Received signal with TR at the target position p_0, b) Received signal with TR at interfering position p_1 (SISO configuration)

TABLE 10 . SPATIAL FOCUSING IN INDOOR ENVIRONMENT (CASE OF: SISO, MISO 2X1 AND MISO3X1)

Configuration	SISO	MISO 2x1	MISO 3x1
$SF_{[dB]}$ (Laboratory type)	5.4	6.5	7.5
$SF_{[dB]}$ (Tunnel type)	6.9	7.7	9.0

A.2.3. Conclusion

This experimental study was performed to assess the characteristics of TR in terms of temporal and spatial focusing. The results show that RT is an interesting candidate for UWB applied to the location. Indeed, not only does TR take advantage of the complexity of the propagation environment, but also it takes advantage of multi-antenna (MISO) to improve focusing. We also found that the best spatio-temporal focusing is obtained for the MISO 3x1 configuration. This configuration is representative of our application as a three transmitting sources and a single receiver are currently considered. In the next section, we will study the contribution of TR-UWB in terms of positioning accuracy.

A.3. Contribution of TR-UWB system in terms of positioning accuracy

A.3.1. Objective

In this last section, we perform a comparative evaluation between a conventional UWB positioning and a TR-UWB positioning system [18]. To compute the 2D receiver position information, we need at least three transmitters. Thus, we consider our previous MISO 3x1 configuration. The operating principle is as follows:

- In the case of the UWB alone system, a sequence of 7 pulses is transmitted by each station to the receiving station. Each transmitter has its own coded signal. The received signals are acquired by the TDS. Post processing evaluates the arrival times of the various signals using a Time Difference of Arrival algorithm (TDOA). Then, the Chan localization algorithm is applied to determine the receiver position [19].

- For the TR-UWB system, each transmitting station sends first a signal which is acquired by the oscilloscope and respectively sent back to the transmitters. The time reversed signals are transmitted from each base station to the receiver. The received signals are then acquired in this TR condition. Then, the same post processing than in the UWB alone system determines the receiver position. However, in this TR configuration, the received signals are correlated with their TR reference signals, and not with the initial UWB sequence.

Experiments were also carried out successively in the anechoic chamber and in the selected indoor environment.

A.3.2. Evaluation in the anechoic chamber

In the anechoic chamber, we consider our five reflector configurations. Three series of acquisition were performed in each case. Fig. 13a and Fig. 13b show an example of the received signals from Tx1 using three reflector plates respectively without TR and with TR. As previously mentioned, a sequence of seven pulses is sent.

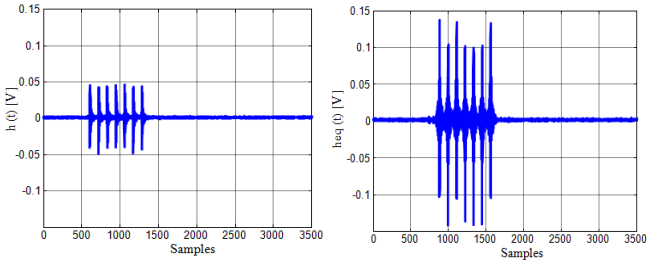

Fig 13. a) Received signal in the case of conventional UWB localization system (without TR); b) Received signal in the case of TR-UWB localization system

After processing, we determine the position of the mobile. Fig. 14 shows the corresponding position errors. With the conventional UWB localization system, we get an error of 11.0 cm, decreasing to 3.3 cm in the case of TR-UWB.

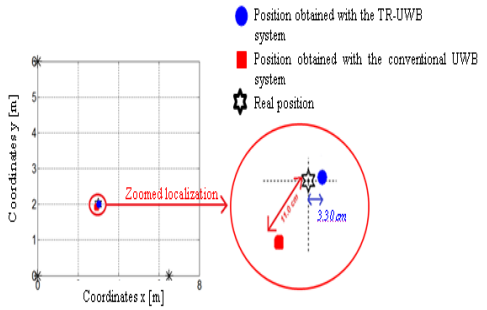

Fig 14. Conventional UWB and TR-UWB localization systems (Scenario with 3 reflector plates in an anechoic chamber)

ISSN: 2277-3754
ISO 9001:2008 Certified
International Journal of Engineering and Innovative Technology (IJEIT)
Volume 3, Issue 12, June 2014

To study the performance of the two systems in our various scenarios, we systematically determined position errors for both UWB and TR-UWB systems. To do this, three sets of acquisition have been exploited and processed and position errors were determined. The results are reported in table 11 and table 12.

TABLE 11 . POSITION ERRORS, UWB ALONE

	Configuration	First set	Second set	Third set
Position error [cm]	Without reflector plates	8.1	8.5	8.2
	1 reflector plate	9.1	9.2	9.2
	2 reflector plates	10.9	11.1	11.3
	3 reflector plates	12.2	12.1	12.1
	4 reflector plates	13.2	13.3	13.4

TABLE 12 .POSITION ERRORS, TR-UWB

	Configuration	First set	Second set	Third set
Position error [cm]	Without reflector plate	8.1	8.0	8.0
	1 reflector plate	7.0	6.9	7.1
	2 reflector plates	5.2	5.4	5.3
	3 reflector plates	3.9	4.0	4.1
	4 reflector plates	3.5	3.6	3.5

The average values obtained for the three acquisitions are reported in table 13 and table 14. Comparing the two systems in the anechoic chamber, without reflector, leads to little difference. Even if the TR-UWB system provides a lower error on localization accuracy, the difference is fairly limited. Of course in a non multipath environment like the anechoic chamber, TR adds little improvement. For all the other considered cases, TR-UWB significantly provides better localization accuracy.

TABLE 13 . AVERAGE POSITION ERROR CONSIDERING THE 3 ACQUISITIONS, UWB ALONE

Number of reflectors	0	1	2	3	4
Position error [cm]	8.3	9.2	11.1	12.1	13.3

TABLE 14 . AVERAGE LOCALIZATION ERROR CONSIDERING THE 3 ACQUISITIONS, TR-UWB

Number of reflectors	0	1	2	3	4
Position error [cm]	8.1	7.1	5.3	4.0	3.5

A.3.3. Evaluation in the indoor environment

The same experimental measurements were repeated using an identical protocol in the case of the indoor environment. Three sets of acquisition were performed. This time, after processing the received signals, we get a position error of 12.9 cm for the conventional UWB system. This error decreases to 6.8 cm with TR-UWB.

A.4. Conclusion

For all the configurations studied and for the all the complex environments considered, we obtained a better positioning accuracy performance using the combination of UWB and TR as compared to the UWB alone technique.

VI. GENERAL CONCLUSION

In this paper, a new system for railway track-to-train, spot communication was analyzed. The proposed balise simultaneously delivers accurate localization information to trains. The equipment can be installed on the side of the track, instead of being set between the rails. The new balise makes use of the association between ultra wide band radio and time reversal technique. Analytical and simulation studies of their characteristics were analyzed. Measurements were also performed in two very different propagation environments, i.e. an anechoic chamber using an added set of metallic reflectors and a tunnel like environment. In all the simulated and experimented configurations, it has been shown, on the one hand, time reversal has major assets to ultra wide band radio in terms of spatio-temporal focusing, and, on the other hand, that this advantage is transferred on the application to the localization. The results obtained allow us to conclude that in all the considered cases, the tracking system provided by time reversal-ultra wide band radio gives better performance compared to ultra wide band radio alone. Using time reversal, a position error below the 10 cm, objective requested for this railway application, was achieved in all cases.

REFERENCES

[1] F. Barber, M. Abril, M. A. Salido, L. P. Ingolotti, P. Tormos, A. Lova, "Survey of automated Systems for Railway Management. Technical report," Universidad Politécnica de Valencia, Department of Information Systems and Computation, 2007.

[2] D. Ke-Lin, M. N. Swamy, "Wireless Communication Systems," ISBN-13: 978-0-521-11403-5, pp. 1020, April 15, 2010.

[3] N. Maaref, P. Millot, X. Ferriéres, C. Pichot, O. Picon, "Electromagnetic Imaging Methode Based On Time Reversal Processing Applied to Through the Wall Target Localization,"

ISSN: 2277-3754
ISO 9001:2008 Certified
International Journal of Engineering and Innovative Technology (IJEIT)
Volume 3, Issue 12, June 2014

Progress In Electromagnetics research M, Vol. 1, pp. 59-67, 2008.

[4] A. F. Molish, "Ultrawideband Propagation Channel-theory, Measurement, and Modelling," Vehicular Technology, IEEE Transaction, Vol. 54, No. 5, pp. 1528-1545, 2005.

[5] M.L. Welbom, "System Considerations for Ultra-Wideband Wireless Networks," IEEE: Radio and Wireless Conference RAWCON2001, Boston, Aug 19-22. 2001, pp.5-8.

[6] H. El-Salabi, P. Kiritsi,, A. Paulraj, G. Papanicolaou, "Experimental Investigation of Time Reversal Precoding for Space-Time Focusing in Wireless Communications," Supported by ONR grant Number N00014-02-1-0088.

[7] D. Porcino, W.Hirt, "Ultra-wideband radio technology: poten-tial and challenges ahead," IEEE Communications Magazine, Vol.41, No. 7, pp. 66–74, Juillet 2003.

[8] W. Suwansantisuk, M. Z. Win, L. A. Shepp "On the performance of wide-bandwidth signal acquisition in dense multipath channels," IEEE Trans. Veh. Technol., vol. 54, No. 5, Sept. 2005, pp. 1584-1594.

[9] L. G. Van Atta, "Electromagnetic Reflector,". U.S. Patent 2 908 002, 1959.

[10] M. Fink, "Ondes et renversement du temps," Bulletin de l'union des professeurs de physique et de chimie, 2005, pp. 25-31.

[11] H. Saghir, M. Heddebaut, F. Elbahhar, A. Rivenq, J.M. Rouvaen, "Time Reversal UWB Wireless Communication-Based train control in tunnel," Journal of communications, vol. 4, No. 4, May 2009, pp. 248-256.

[12] ETSI TR 101 538, "Electromagnetic compatibility and Radio Spectrum Matters (ERM); Short Range Devices (SRD); UWB location traking devices in the railroad environment," Technical Report V1.1.1, October 2012.

[13] A. Derode, P. Roux and M. Fink, "Robust acoustic time reversal with high order multiple scattering," Physical review letters, Vol. 75, No. 23, 1995, pp 4206-4209.

[14] B. E. Henty and D.D. Stancil, "Multipath-Enabled Super-Resolution for RF and Microwave Communication using Phase-conjugate Arrays," Phy-Rev. Lett, Vol.93, No.24, 2004, pp. 1-4.

[15] G. Lerosey, J. de Rosny, A. Tourin, A. Derode, G, Montaldo, M. Fink, "Time Reversal of Electromagnetic waves," Physical review letters, Vol. 92, No. 19.2004, pp. 1-3.

[16] X. Liu, B.-Z. Wang, S. Xiao, J. Deng, "Performance of Impulse Radio UWB Communication Based On Time Reversal Technique," Progress In Electromagnetics Research, PIER Vol.79, No. 11, 2008, pp. 401-413.

[17] D. Abassi-Moghadam, D. Tabataba Vakili, "Channel characterization of time reversal UWB communication systems," Wiley International Journal of Communication Systems, Vol. 65, No.9-10, 2010, pp 601-614.

[18] B. Fall, M. F. Elbahhar, M. Heddebaut, A. Rivenq, "Time-Reversal UWB Positioning Beacon for Railway Application," International Conference on Indoor Positioning and Indoor Navigation (IPIN), IEEE Proceeding, Sydney (Australia), 2012, pp.1-8.

[19] Y.T. Chan, 1994. "A Simple and Efficient Estimator For Hyperbolic Location," IEEE Transactions on Signal Processing, 1905-1915.

AUTHOR'S PROFILE

Bouna Fall was born in 1983. He received the M.S and Ph.D. degrees from the University of Valenciennes (France) in 2009 and 2013, respectively. Currently he is assistant research at this university. His primary interest is in signal processing especially Ultra Wideband technology and Time reversal techniques applied to communication and localization systems.

Fouzia Elbahhar Boukour was born in 1975. She received the M.S and Ph.D. degrees from the University of Valenciennes (France) in 2000 and 2003, respectively. She is now employed as researcher at IFSTTAR/LEOST, Villeneuve d'Ascq, France. She is involved in signal processing especially Ultra Wideband technology. Her major research interests are signal processing localization and communication techniques especially for land transportation like communication Vehicle to Vehicle and vehicle to infrastructure and localization systems.

Marc Heddebaut was born In Somain, France, in 1955. He received the M.S. and Ph.D. degrees in electronics from the University of Lille France in 1980 and 1983, respectively. He joined the French National Institute for Transportation and Safety Research (INRETS now IFSTTAR) in 1983 and became A senior researcher in 1988. Since 1979, he has been working in the field of land mobile communication and electromagnetic compatibility. His primary interests include telecommunication and radar systems dedicated to land transport, EMC, mobile localization and command control of automated vehicles.

Atika Rivenq-Menhaj was born in 1970. She received her Diploma of Engineering and the M.S j degree in 1993 and then her Ph.D. degree in1996, from the University of Valenciennes (France). She is now Professor in electronics at this university. Her primary interest is in signal processing applied to intelligent transportation systems and telecommunication systems